https://doi.org/10.1061/(ASCE)ST.1943-541X.0002343

ST7442

Cold-Formed Lean Duplex Stainless Steel Tubular Members under Concentrated Interior Bearing Loads

Yancheng Cai M.ASCE[1] and Ben Young, F.ASCE[2]

ABSTRACT

In this study, a total of 58 tests were performed on cold-formed lean duplex stainless steel (LDSS) tubular members that under three different loading conditions of concentrated interior bearing forces. The loading conditions included Interior-One-Flange (IOF), Interior-Two-Flange (ITF) and interior loading (IL). The loading conditions of IOF and ITF are specified in the American and Australian/New Zealand cold-formed stainless steel design specifications, while the loading condition of IL simulated the floor joist members positioned on a solid foundation subjected to concentrated bearing load. The cold-formed LDSS specimens were failed by web crippling. The test strengths were compared with the nominal strengths predicted by the international specifications for stainless steel structures. In addition, the strengths predicted by the North American Specification for cold-formed carbon steel structures and using the design equations proposed in the literature for cold-formed duplex stainless steel members were also compared with the test strengths. It was found that the nominal strengths predicted by the international specifications for stainless steel structures are conservative and reliable for the cold-formed LDSS members under concentrated interior bearing loads. The predictions by the North American Specification were generally unconservative and not reliable, while the predictions

[1] Post-doc Fellow, Dept. of Civil Engineering, Univ. of Hong Kong, Pokfulam Rd., Hong Kong (corresponding author). Email: yccai@hku.hk

[2] Professor, Dept. of Civil and Environmental Engineering, The Hong Kong Polytechnic Univ., Hong Kong. Email: ben.young@polyu.edu.hk

(Formerly, Dept. of Civil Engineering, The Univ. of Hong Kong, Pokfulam Rd., Hong Kong. Email: young@hku.hk)

from the literature were generally less conservative and reliable compared with those predicted by the stainless steel design specifications.

Keywords: Cold-formed lean duplex stainless steel; Concentrated bearing loads, Experimental investigation; Web crippling failure

INTRODUCTION

Lean duplex stainless steel (LDSS), including EN 1.4062 and EN 1.4162, is a relatively new material, and has recently gained significant attention in construction industry due to its exceptional mechanical properties, good corrosion resistance and lower cost compare to its counterpart of duplex stainless steel type. In the past few years, significant progress has been made on the behavior of LDSS structural members, including material properties (Huang and Young 2012), beams (Huang and Young 2014a, Saliba and Gardner 2013a, Theofanous and Gardner 2010), columns (Theofanous and Gardner 2009, Huang and Young 2013, 2014b), beam-columns (Huang and Young 2014c-d), plate girders (Saliba and Gardner 2013b, Saliba el al. 2014), and LDSS bolted connections (Cai and Young 2014). Furthermore, bearing resistance design rules were proposed for LDSS double shear bolted connections (Cai and Young 2016) and single shear bolted connections (Cai and Young 2018a).

Web crippling strength of stainless steel tubular sections should be checked carefully as the sections may cripple under high concentrated bearing loads. Investigations on web crippling failure of cold-formed stainless steel were carried out in lipped channel sections (Korvink and van den Berg 1994, Korvink et al. 1995), and tubular sections (Talja and Salmi 1995, Gardner et al. 2006). Zhou and Young (2006, 2007a-b) conducted a series of tests on web crippling of cold-formed austenitic and duplex stainless steel tubular sections, that covered to the loading conditions of End-Two-Flange (ETF), Interior-Two-Flange (ITF), End-One-Flange (EOF),

Interior-One-Flange (IOF), end loading (EL) and interior loading (IL). In addition, the cold-formed ferritic stainless steel tubular sections that subjected to web crippling were investigated by Bock et al. (2013) and Li and Young (2017). More recently, the web crippling behaviour of cold-formed LDSS tubular sections subjected to concentrated end bearing loads (loading conditions of EOF, ETF and EL) were experimentally investigated by Cai and Young (2019). However, up to date, there is no investigation on cold-formed LDSS tubular members under concentrated interior bearing loads (loading conditions of IOF, ITF and IL), which is the focus of this study.

The web crippling design rules are specified in the current international stainless steel specifications, i.e., American Society of Civil Engineers Specification (ASCE, 2002), Australian/ New Zealand Standard (AS/NZS, 2001) and European Code (EC3-1.4, 2015). However, it should be noted that the web crippling design rules in these stainless steel specifications are mainly adopted from those for carbon steel members. Furthermore, the cold-formed LDSS is not covered in the current ASCE (2002) and AS/NZS (2001) specifications, while it was recently introduced in the EC3-1.4 code (2015). It should be noted that EC3-1.4 (2015) does not have specific design rules for web crippling design and may refer to those specified in the EC3-1.3 code (2006), which is for cold-formed carbon steel sections.

Totally 58 tests of cold-formed LDSS members subjected to concentrated interior bearing loads were conducted. The LDSS members including EN 1.4062 and EN 1.4162, had square and rectangular hollow sections. The tests were conducted under three concentrated interior bearing loads, namely, the loading conditions of IOF, ITF and IL. The loading conditions of IOF and ITF are specified in the ASCE (2002) and AS/NZS (2001) specifications, while the loading condition of IL simulated the floor joist members subjected to concentrated bearing load. The test LDSS

specimens were failed by web crippling. The test strengths were compared with the nominal strengths predicted by the ASCE (2002), AS/NZS (2001) and EC3-1.4 (2015) specifications for stainless steel structures. In addition, the web crippling strengths predicted by the North American Specification (NAS) (2016) for cold-formed carbon steel structures and using the design equations proposed by Zhou and Young (2008) for cold-formed duplex stainless steel tubular sections were also compared with the test strengths. The reliability of the aforementioned web crippling design provisions was assessed by reliability analysis.

EXPERIMENTAL INVESTIGATION

Test Specimens and bearing plates

A total of 58 cold-formed LDSS tubular members were tested, including nine square and rectangular hollow sections. The LDSS has two grades of EN 1.4062 and EN 1.4162. The measurements on the dimensions of the cross-sections were recorded. These include the height of web (H), width of flange (B), the section thickness (t) and the section inner radius (r_i). The values of measured web heights were in the range of 19.9 to 152.1 mm, flange widths in the range of 20.3 to 152.4 mm, thicknesses in the range of 1.49 to 3.10 mm, and inner radii in the range of 0.8 to 6.5 mm. In addition, the web slenderness ratios (h/t) ranged from 9.7 to 43.3. The test specimens with the measured dimensions are shown in Tables 1-3, with the nomenclature of the section defined in Fig. 1. The length (L) of the specimen was designed by referring to the NAS (2016) and the measured values are also shown in Tables 1-3. For the loading condition of IOF, the clear distance of 1.5H was designed between the bearing edges of adjacent opposite concentrated loads or reactions; while for the loading conditions of ITF and IL, the similar 1.5H clear distance was designed but from the specimen end to the bearing plate edge, as illustrated in Figs. 2(a)-2(c).

Steel bearing plates were used to transfer the applied loading or reaction into the specimens. A total of six steel bearing plates with 50 mm thickness having different dimensions were produced. The steel bearing plates were long and wide enough to cover the full section flange width, except for the rounded corners. Generally, two bearing lengths were used for each section. Hence, the effect of different bearing lengths was also investigated. In this experimental investigation, all flanges of the cold-formed LDSS tubular members were not fastened to the steel bearing plates.

Specimen Labelling and Material Properties

The LDSS test specimens were labelled in order to identify the loading conditions (IOF, ITF and IL), nominal section dimensions as well as the bearing length, as shown in Tables 1-3. For examples, the specimens of "IOF80×150×3.0N60", "ITF80×150×3.0N60" and "IL80×150×3.0N150-r" represent the following. The two or three letters in the front of the label mean that the cold-formed LDSS tubular section was tested under the interior loading condition of Interior-One-Flange (IOF), Interior-Two-Flange (ITF) or Interior loading (IL). The next segment shows the nominal dimension of the specimen section (H×B×t), namely, 80×150×3.0 means H = 80 mm, B = 150 mm and t = 3.0 mm. The last segment N60 or N150 means that the specimen was subjected to a bearing length of 60 or 150 mm. The repeated test was indicated by the last letter "r" in the label.

Tensile coupon and compressive coupon specimens were tested. Both the coupon specimens and the specimens under interior concentrated bearing loads were cut from the same batch of LDSS tubes. The tensile coupon specimens were cut from the tubular sections in the longitudinal direction, while the compressive coupon specimens were extracted in the transverse direction from the webs (Cai and Young 2019). Strain gauges were used to measure the strain of the tensile and compressive coupons. The tensile and compressive coupon tests were conducted in

accordance with the procedure suggested by Huang and Young (2014e) and Li and Young (2017), respectively. A data acquisition system was used to record the load and strain at regular intervals during the coupon tests. The details of the tensile and compressive coupon tests were described in Cai and Young (2019). Table 4 illustrates the material properties obtained from the tensile and compressive coupons, including Young's modulus (E^T *and* E^C), static 0.2% proof stress ($f_{0.2}^T$ *and* $f_{0.2}^C$) and static tensile strength (f_u^T).

Test Rig and Operation

Tests of the cold-formed LDSS tubular hollow sections were conducted by three different concentrated interior bearing loads, namely the loading conditions of IOF, ITF and IL. The loading conditions of IOF and ITF are specified in the ASCE (2002) and AS/NZS (2001) stainless steel specifications, while the loading condition of IL simulated the floor joist members on a solid foundation subjected to concentrated bearing load. The loading condition of IL is not specified in the ASCE (2002) and AS/NZS (2001) specifications.

For the loading condition of IOF, the aforementioned steel bearing plate was positioned at the mid-span of the test specimen. The steel bearing plate was fixed to a half round, and it transferred the applied load to the top flange of specimen. At the test specimen ends, two steel load transfer plates having the same width and thickness of the steel bearing plate were positioned. The steel load transfer plates were supported by two identical rollers in order to provide symmetrical support. Steel stiffening plates were used to prevent web failure of the specimen at the ends. They were set at both sides of the specimen. In the mid-span of the test specimen, two calibrated linear variable displacement transducers (LVDTs) were used to measure the vertical web deformation of the specimen. Another two LVDTs had flat plastic plates at the ends were positioned at both sides of the specimen webs in the mid-span. It should

be noted that the plastic plates rigidly connected to the ends of the LVDTs. The plastic plates covered the specimen webs in an area that was able to capture the maximum deformations in lateral direction. The average readings of the two LVDTs were used for the vertical and lateral web deformation, respectively. The test set up of Specimen IOF150×80×3.0N90 is illustrated in Fig. 3(a), with the corresponding schematic view as shown in Fig. 2(a).

For the loading condition of ITF, the test specimen in the mid-length was loaded by using two identical steel bearing plates. The steel bearing plates were positioned at the top and bottom flanges of the specimen. The steel bearing plates were fixed to the two half rounds. The applied load was transferred to the specimen flanges by the steel bearing plates through half rounds. Four calibrated LVDTs were used to measure the vertical web deformations of the test specimen. The lateral web deformations of the test specimen were measured in a similar way as those for the IOF loading condition. The test setup of Specimen ITF80×150×3.0N150 under ITF loading condition is illustrated in Fig. 3(b), with the corresponding schematic view as shown in Fig. 2(b).

While for the IL loading condition, only one steel bearing plate was used. The steel bearing was fixed to a half round and positioned on the top flange of the test specimen in the mid-length to transfer the applied concentrated load. The arrangements of the LVDTs for the measurements of vertical web deformations and lateral web deformations are identical to those for the measurements in the ITF loading condition. The test setup and schematic view for Specimen IL100×100×3.0N30 subjected to IL loading condition are shown in Fig. 3(c) and Fig. 2(c), respectively, where the specimen was positioned on a fixed flat solid base plate.

The compressive force was applied to the test specimens by a load testing machine. The tests were carried out by displacement control. The loading rate of 0.3 mm/min was used for all the

tests. The applied load from the machine and the readings from the LVDTs were recorded by a data acquisition system regularly during the tests.

Test Results

Tables 1-3 reported the test strengths per web (P_{test}), for the cold-formed LDSS specimens under the loading conditions of IOF, ITF and IL, respectively. All the LDSS tubular sections under the concentrated interior bearing loads were failed by web crippling. Repeated tests were conducted on specimens that covered the three different loading conditions, namely, specimens IOF50×20×1.5N30, IOF100×100×3.0N90, ITF20×50×1.5N30, ITF50×20×1.5N30, ITF60×40×2.0N30, ITF60×120×3.0N90, ITF80×150×3.0N150, IL40×60×2.0N60, IL50×20×1.5N30, IL60×40×2.0N50 and IL80×150×3.0N150. The differences between the first and repeated test strengths were within 2.0%. The relatively small differences demonstrated that the test results were reliable. Figs. 4(a)-(b) exemplifies the load versus the web deformation curves for specimens IOF150×80×3.0N90, ITF60×40×2.0N30 and IL80×150×3.0N60. The vertical axis represents the applied load on the specimen, while the horizontal axis plots the measured vertical and horizontal deformation of the specimen. The web crippling failure of specimens IOF80×150×3.0N60, ITF80×150×3.0N150 and IL100×100×3.0N30 that subjected to different concentrated interior bearing loads is illustrated in Figs. 5(a)-(c).

DESIGN RULES

The design rules for sections failed by web crippling are provided in the current international design specifications for stainless steel structures (ASCE 2002, AS/NZS 2001, EC3-1.4 2015). The design rules in the AS/NZS Standard (2001) and the ASCE Specification (2002) are identical. Hence, the web crippling design strengths predicted by the ASCE (2002) and the AS/NZS (2001) specifications are identical. The web crippling design rules in the EC3-1.4 (2015)

may refer to those specified in the EC3-1.3 Code (2006). In this study, the EC3-1.3 Code (2006) was used to calculate the web crippling strengths of the cold-formed LDSS sections. In addition, the web crippling design rules specified in the NAS (2016) were used, although the design specification is focused on cold-formed carbon steel structural members. This is because, as mentioned earlier in the "Introduction", the web crippling design provisions in the current stainless steel specifications are mainly adopted from those design provisions for carbon steel structures. The web crippling design rules proposed by Zhou and Young (2008) for cold-formed duplex stainless steel hollow sections were also assessed, as the grade of LDSS is close to that of duplex stainless steel.

In the ASCE Specification (2002), the web crippling design rules for the sections with flanges stiffened or partially stiffened that subjected to loading conditions of IOF and ITF are specified in Section 3.3.4 of the specification. The design rules are applicable to sections with single webs or similar sections, and hence were used for the tubular hollow sections due to the similarity in this study. Noted that the current ASCE (2002) or AS/NZS (2001) specification does not specify design rules for IL loading condition. Hence, the web crippling design for specimens under the loading condition of IL used the same equations as those in the loading conditions of IOF and ITF in this study.

In EC3-1.3 code (2006), the web crippling resistance is referred as the local transverse resistance. The design rules specified in Section 6.1.7.3 with the Equation 6.18 of the EC3-1.3 (2006) are applicable to sections with two or more unstiffened webs. Tubular sections belong to sections with two or more unstiffened webs. Hence, the design rules in Section 6.1.7.3 with the Equation 6.18 were adopted in this study. The values of the web crippling coefficient α and the effective bearing length l_a depend on the loading conditions as illustrated in Fig. 6.9 of EC3-1.3 (2006)

and shape of the section, i.e. sheeting profiles, liner trays and hat sections. The IOF, ITF and IL loading conditions in this study belongs to Category 1 according to the Fig. 6.9 of the EC3-1.3 (2006). Hence, α and l_a were chosen as 0.057 and 10 mm, respectively, in the calculation of nominal strength P_{EC} predicted by EC3-1.3 (2006). It should be noted that the EC3-1.3 (2006) does not take into consideration of the web slenderness ratio and uses the same bearing length of 10 mm for the design. Even though the LDSS specimen sections had different web slenderness, and were loaded by steel bearing plates with different bearing lengths in the range of 30 to 150 mm in this study.

In the NAS Specification (2016), the web crippling design rules of sections with single web having stiffened or partially stiffened flanges are specified in Section G5 with a unified design equation. The unified design equation is suitable for sections under different loading conditions, including ITF and IOF. Zhou & Young (2008) proposed new coefficients for the unified equation specified in the NAS (2016) for web crippling of cold-formed austenitic and duplex stainless steel tubular structural members. The proposed design equation (Zhou and Young 2008) is suitable for web crippling of cold-formed austenitic and duplex stainless steel tubular sections under the loading conditions of ETF, ITF, EOF, IOF, EL and IL. However, the cold-formed LDSS sections are not covered by Zhou and Young (2008). The unified equation is shown in the following:

$$P = Ct^2 f_y \sin\theta \,(1 - C_R\sqrt{\frac{r}{t}})(1 + C_N\sqrt{\frac{N}{t}})(1 - C_h\sqrt{\frac{h}{t}}) \quad (1)$$

where P is the nominal web crippling strength per web, C = overall web crippling coefficient; C_R = inside corner radius coefficient; C_N = bearing length coefficient; C_h = web slenderness coefficient. The coefficients in Equation (1) are shown in Table 5 of this paper. In addition, the resistance factors (ϕ) for web crippling design strength under different loading conditions as

recommended by NAS (2016) and Zhou and Young (2008) are also specified in Table 5. Similar to the ASCE (2002) and AS/NZS (2001) specifications, it should be noted that the NAS (2016) does not provide design rules for IL loading condition. Hence, the web crippling design for specimens under loading condition of IL used the same equation as those for the loading conditions of IOF and ITF in this study.

RELIABILITY ANALYSIS

Reliability analysis was performed for the web crippling design rules used in this study. The analysis was performed in accordance with those specified in the Commentary of the ASCE Specification (2002) for cold-formed stainless steel members. The aforementioned web crippling design provisions in the ASCE (2002), EC3-1.4 (2015) that referred to EC3-1.3 (2006) for stainless steel structures, as well as those specified in the NAS (2016) for cold-formed carbon steel and Zhou and Young (2008) for cold-formed duplex stainless steel were examined. It should be noted that the reliability analysis for the design provisions in the EC3-1.3 (2006) should follow the Eurocode 0 (2005). For direct comparison, the reliability analysis that specified in the ASCE (2002) was used in this study.

In this study, the reliability index (β) greater than or equal to 2.5 was set for the design provisions being considered reliable and probabilistically safe. The resistance factors (ϕ) for web crippling design strength as recommended by the ASCE (2002), EC3-1.4 (2015), NAS (2016) and Zhou and Young (2008) are shown in Tables 6-8. The load combination of 1.2DL + 1.6LL was used to determine the reliability index for the ASCE (2002), NAS (2016) and Zhou and Young (2008), while combination of 1.35DL + 1.5LL was used for European code (2015), where DL represents the dead load while LL represents the live load. The ratio of 0.2 for DL/LL is used in the commentary of the ASCE (2002). The statistical parameters suggested in Section 6.2 of

ASCE (2002) were used, where M_m = 1.10, F_m = 1.00, V_M = 0.10 and V_F = 0.05, which are the mean values and coefficients of variation of material factor and fabrication factor, respectively. In addition, the mean value (P_m) and the coefficients of variation (V_P) of tests to the design prediction ratios are shown in Tables 6-8. A correction factor (C_P) in the Section K2 of the NAS (2016) was used in this study to take into consideration of the influence of limited number of test data, where $C_P = (1+1/n)m/(m-3)$, in which n is the number of tests and m ($m = n-1$) is the degrees of freedom. The reliability index (β) for the cold-formed LDSS tubular members under concentrated interior bearing loads were calculated, and reported in Tables 6-8, for the loading conditions of IOF, ITF and IL, respectively.

COMPARISON OF TEST STRENGTHS WITH PREDICTED STRENGTHS

The experimental strengths (P_{test}) per web that subjected to the three different concentrated interior bearing loads were compared with the nominal strengths predicted by the stainless steel specifications (ASCE 2002, AS/NZS 2001, EC3-1.4 2015), the cold-formed carbon steel specification (NAS 2016), as well as Zhou and Young (2008) for web crippling design of cold-formed duplex stainless steel section. Note that the design rules in EC3-1.4 (2015) refers to those specified in EC3-1.3 (2006), and the AS/NZS Standard (2001) has adopted the ASCE Specification (2002) for the design of web crippling strength. Therefore, the predicted values are identical for the AS/NZS (2001) and the ASCE (2002) specifications.

The test strengths (P_{test}) per web were compared with the predicted strengths for the IOF, ITF and IL loading conditions as shown in Tables 6-8, respectively. The nominal strengths predicted by the ASCE (2002), EC3-1.3 (2006), NAS (2016) specifications as well as Zhou and Young (2008) are included in each table. The predicted strengths were calculated using the measured cross-section dimensions as shown in Tables 1-3. In addition, the measured material properties

were used in the calculation, including the Young's moduli (E^T and E^C) and the corresponding static 0.2% proof stresses ($f_{0.2}^T$ and $f_{0.2}^C$) that obtained from the longitudinal tensile and transverse compressive coupons, as shown in Table 4. The predicted strengths P^T and P^C were calculated using the material properties obtained from the longitudinal tensile and compressive coupons, respectively.

Using the material properties of E^T and the corresponding static $f_{0.2}^T$ for the nominal strengths predictions (P^T), for the loading condition of IOF, the P_m values of P_{test}/P_{ASCE}^T, P_{test}/P_{EC}^T, P_{test}/P_{NAS}^T and $P_{test}/P_{Z\&Y}^T$ are 1.12, 2.61, 0.87 and 1.13, with the corresponding COVs of 0.115, 0.135, 0.097 and 0.095, for the ASCE (2002), EC3-1.3 (2006), NAS (2016) specifications and Zhou and Young (2008) predictions, respectively; and the corresponding values of β are 3.66, 5.45, 1.85 and 3.81, as shown in Table 6. For the loading condition of ITF, the P_m values are 1.05, 5.94, 0.88 and 1.15 for P_{test}/P_{ASCE}^T, P_{test}/P_{EC}^T, P_{test}/P_{NAS}^T and $P_{test}/P_{Z\&Y}^T$, with the corresponding COVs of 0.197, 0.171, 0.307 and 0.117; and the corresponding β of 2.89, 7.81, 1.50 and 3.74, as shown in Table 7. In addition, Table 8 illustrates the comparison results for the loading condition of IL. In this case, the P_m values of P_{test}/P_{ASCE}^T, P_{test}/P_{EC}^T, P_{test}/P_{NAS}^T and $P_{test}/P_{Z\&Y}^T$ are 1.41 (1.17), 3.27, 1.05 (0.92) and 1.05, with the corresponding COVs of 0.212 (0.223), 0.216, 0.136 (0.276) and 0.137; and the corresponding values of the β are 3.68 (3.03), 6.05, 2.40 (1.72) and 2.80. It should be noted that the predicted strengths for IL loading condition used the same equations as those for IOF (ITF) loading conditions for both ASCE (2002) and NAS (2016) in this study, as shown in Table 8.

Overall, it was found that the nominal strengths predicted by the stainless steel design specifications (ASCE 2002, AS/NZS 2001, EC3-1.4 2015) are conservative and reliable for the three different loading conditions. The predicted strengths by the European stainless steel codes

(EC3-1.4 2015) are much more conservative than those predicted by the ASCE stainless steel specification (2002), as shown in Tables 6-8. This is because that the European codes (2006, 2015) do not take into consideration of the web slenderness ratio although the LDSS specimen sections had different web slenderness in this study. Furthermore, the bearing length of 10 mm was used in the calculation for the three different loading conditions of IOF, ITF and IL, although the specimen sections were loaded by different bearing length from 30 to 150 mm. However, it should be noted that the web crippling design equations in ASCE (2002), AS/NZS (2001), NAS (2016) and Zhou and Young (2008) consider the web slenderness ratio *h/t* and use the actual bearing length *N* in the calculation. In addition, the web crippling design rules for stainless steel in EC3-1.4 (2015) refer to those for carbon steel in EC3-1.3 (2006), as mentioned previously. It is found that the nominal strengths predicted by the NAS (2016) are generally un-conservative compared with the test strengths, except for the IL loading condition where the IOF design equation was used, as shown in Tables 6-8. The NAS predictions are shown to be not reliable as the values of reliability index (β) are smaller than 2.5. The predictions by ASCE (2002) and Zhou and Young (2008) are averagely 12% higher than the test strengths for IOF loading condition. The ASCE (2002) provides less conservative predictions in average for the ITF loading condition, i.e., 1.05 of P_m for P_{test}/P_{ASCE}^T compared with 1.15 of P_m for $P_{test}/P_{Z\&Y}^T$; however, predictions by Zhou and Young (2008) are better than those by ASCE (2002) for the IL loading conditions, e.g., 1.41 (1.17) of P_m for P_{test}/P_{ASCE}^T compared with 1.05 of P_m for $P_{test}/P_{Z\&Y}^T$. This may be due to the current ASCE (2002) specification does not specify design rules for IL loading condition. Both the predictions by ASCE (2002) and Zhou and Young (2008) are reliable for the three different interior loading conditions as the values of reliability index (β) are larger than 2.5.

The predicted strengths using the material properties of E^C and the corresponding static 0.2% proof stress of $f_{0.2}^C$ were also calculated and compared as shown in Tables 6-8. Generally, the predictions are less conservative, or even not conservative compared with those predicted using the material properties of longitudinal tensile coupon tests, for the cold-formed LDSS subjected to concentrated interior bearing loads, i.e., IOF, ITF and IL loading conditions. This is because the 0.2% proof stress (yield strength) obtained from the transverse compressive coupon tests are generally higher than those obtained from the longitudinal tensile coupon tests due to the cold-forming process of the sections, where the transverse direction of the tubes undergoes more cold work than the longitudinal direction as a result of the transverse bending.

The comparisons of tested-to-predicted strengths using material properties from longitudinal tensile coupon tests and transverse compression coupon tests are shown in Figs. 6(a)-(d) for ASCE (2002), EC3-1.4 (2015), NAS (2016) and Zhou & Young (2008), respectively. The three different concentrated interior bearing load conditions (IOF, ITF and IL) in which the cold-formed LDSS sections tested were included in each figure. The vertical axis plots the test strengths per web while the horizontal axis represents the predicted strengths per web. In Figs. 6(a)-(d), the results calculated using the material properties in tensile and compression were identified by "(T)" and "(C)" in the top right hand side of the label legend, respectively. Note that the predicted strengths for the loading condition of IL adopted the design rules of IOF and ITF loading conditions for both ASCE (2002) and NAS (2016) in this study, and they are also identified as shown in Figs. 6(a) and (c).

CONCLUSIONS

A test program on cold-formed lean duplex stainless steel (LDSS) tubular members, including EN 1.4062 and EN 1.4162, under concentrated interior bearing loads were conducted. The

members of square and rectangular hollow sections were investigated. The variation of parameters in the test specimens mainly included the ratio of web to thickness in the sections and the bearing lengths that acted on the members through the steel bearing plates. The tubular sections were tested under three different loading conditions of concentrated interior bearing loads, namely, the Interior-One-Flange (IOF), the Interior-Two-Flange (ITF) and interior loading (IL). The loading conditions of IOF and ITF were specified in the ASCE (2002) and AS/NZS (2001) for the design of cold-formed stainless steel structural members, while loading condition of IL simulated the floor joist members positioned on a solid foundation subjected to concentrated bearing load. Web crippling failure mode was observed for all the test specimens.

The test strengths and the nominal strengths were compared, in which the nominal strength were calculated from the ASCE (2002), AS/NZS (2001) and EC3-1.4 (2015) for stainless steel structures. Furthermore, the design rules specified in the NAS (2016) for cold-formed steel structures and those proposed by Zhou and Young (2008) for web crippling of cold-formed duplex stainless steel tubular sections were also examined. In the calculation of nominal strengths, both the material properties obtained from longitudinal tensile coupon tests and compressive coupon tests were used. Reliability analysis was performed to examine the reliability of the aforementioned design rules.

Using the material properties of the longitudinal tensile coupons, it was found that the nominal strengths predicted by the ASCE (2002), EC3-1.4 (2015) and Zhou and Young (2008) for stainless steel structures are conservative and reliable for the cold-formed LDSS subjected to the three different concentrated interior bearing loads, whereas the predictions from the EC3-1.4 (2015) are more conservative. The predictions by NAS (2016) are generally unconservative and not reliable. The predictions by ASCE (2002) and Zhou and Young (2008) are generally less

conservative and reliable compared with those predicted by the stainless steel design specification (EC3-1.4 2015). Using the material properties of the transverse compressive coupons, the predictions are generally less conservative or even unconservative compared with those predicted by using material properties of longitudinal tensile coupon tests for the cold-formed LDSS subjected to concentrated interior bearing loads with the loading conditions of IOF, ITF and IL.

ACKNOWLEDGMENTS

The authors are grateful to STALA Tube Finland for providing the test specimens. The research work described in this paper was supported by a grant from the Research Grants Council of the Hong Kong Special Administrative Region, China (Project No. HKU17209614E). The authors are also grateful to Miss Ning Yan CHAN for her assistance in the experimental program as part of her final year undergraduate research project at the University of Hong Kong.

REFERENCES

ASCE (2002). "Specification for the design of cold-formed stainless steel structural members". SEI/ASCE-8-02, Reston, VA: ASCE.

AS/NZS (2001). "Cold-formed stainless steel structures." AS/NZS 4673:2001, Australian/New Zealand Standard (AS/NZS), Standards Australia, Sydney, Australia.

Bock, M., Arrayago, I., Real, E. and Mirambell, E. (2013). "Study of web crippling in ferritic stainless steel cold formed sections." Thin-Walled Structures, 69, 29–44.

Cai, Y. and Young, B. (2014). "Structural behavior of cold-formed stainless steel bolted connections." Thin-Walled Structures, 83, 147-156.

Cai, Y. and Young, B. (2016). "Bearing factors of cold-formed stainless steel double shear bolted connections at elevated temperatures." Thin-walled Structures, 9, 212-219.

Cai, Y. and Young, B. (2018a). “Fire resistance of stainless steel single shear bolted connections.” Thin-Walled Structures, 130, 332-346.

Cai, Y. and Young, B. (2019). “Web crippling of lean duplex stainless steel tubular sections under concentrated end bearing loads.” Thin-Walled Structures, 134, 29-39.

EC0. (2005). “Eurocode 0: basis of structural design.” EN 1990:2002+A1:2005. Brussels, Belgium: European committee for standardization.

EC3-1.4. (2015). “Eurocode 3. Design of steel structures - Part 1.4: General rules - Supplementary rules for stainless steels.” EN 1993-1-4:2006+A1:2015, Brussels, Belgium, European Committee for Standardization.

EC3-1.3. (2006). “Eurocode 3: Design of steel structures - Part 1–3: General rules – Supplementary rules for cold-formed members and sheeting.” EN 1993-1-3, Brussels, Belgium: European committee for standardization.

Gardner, L., Talja, A. and Baddoo, N.R. (2006). “Structural design of high-strength austenitic stainless steel.” Thin-Walled Structures, 44, 517–528.

Huang, Y. and Young, B. (2012). “Material properties of cold-formed lean duplex stainless steel sections.” Thin-Walled Structures, 54, 72-81.

Huang, Y. and Young, B. (2013). “Tests of pin-ended cold-formed lean duplex stainless steel columns.” Journal of Constructional Steel Research, 82, 203-215.

Huang, Y. and Young, B. (2014a). “Experimental and numerical investigation of cold-formed lean duplex stainless steel flexural members.” Thin-Walled Structures, 73, 216-228.

Huang, Y. and Young, B. (2014b). “Structural performance of cold-formed lean duplex stainless steel columns.” Thin-Walled Structures, 83, 59-69.

Huang, Y. and Young, B. (2014c). “Experimental investigation of cold-formed lean duplex stainless steel beam-columns.” Thin-Walled Structures, 76, 105-117.

Huang, Y. and Young, B. (2014d). “Design of cold-formed lean duplex stainless steel members in combined compression and bending.” Journal of Structural Engineering, 141, 5, 04014138.

Huang, Y. and Young, B. (2014e) “The art of coupon tests.” Journal of Constructional Steel Research, 96, 159-175.

Korvink, S.A. and van den Berg, G.J. (1994). “Web crippling of stainless steel cold-formed beams.” Proc., 12th International Specialty Conference on Cold-Formed Steel Structures, University of Missouri–Rolla, St. Louis, MO.

Korvink, S.A., van den Berg, G.J. and van der Merwe, P. (1995). “Web crippling of stainless steel cold-formed beams.” Journal of Construction Steel Research, 34, 225–248.

Li, H-T. and Young, B. (2017). “Cold-formed ferritic stainless steel tubular structural members subjected to concentrated bearing loads.” Engineering Structures, 145, 392-405.

NAS (North American Specification). (2016). “North American Specification for the design of cold-formed steel structural members.” NAS AISI S100–16, Washington DC: American Iron and Steel Institute (AISI).

Saliba, N. and Gardner, L. (2013a). “Cross-section stability of lean duplex stainless steel welded I-sections.” Journal of Constructional Steel Research, 18, 1-14.

Saliba, N. and Gardner L. (2013b). “Experimental study of the shear response of lean duplex stainless steel plate girders.” Engineering Structures, 46, 375-391.

Saliba N., Real, E., Gardner, L. (2014). “Shear design recommendations for stainless steel plate girders.” Engineering Structures, 59, 220-228.

Talja, A. and Salmi, P. (1995). “Design of stainless steel RHS beams, columns and beam-columns.” Research note 1619, VTT Building Technology, Finland.

Theofanous, M. and Gardner L. (2009). “Testing and numerical modelling of lean duplex stainless steel hollow section columns.” Engineering Structures, 31, 3047-3058.

Theofanous, M. and Gardner L. (2010). “Experimental and numerical studies of lean duplex stainless steel beams.” Journal of Constructional Steel Research, 66, 816-825.

Zhou, F. and Young, B. (2006). “Cold-formed stainless steel sections subjected to web crippling.” Journal of Structural Engineering, 132, 1, 134-144.

Zhou, F. and Young, B. (2007a). “Cold-formed high-strength stainless steel tubular sections subjected to web crippling.” Journal of Structural Engineering, 133, 3, 368–377.

Zhou, F. and Young, B. (2007b). “Experimental and numerical investigations of cold-formed stainless steel tubular sections subjected to concentrated bearing loads.” Journal of Constructional Steel Research, 63, 11, 1452-1466.

Zhou, F. and Young, B. (2008). “Web crippling of cold-formed steel tubular sections.” Advances in Structural engineering, 11, 6, 679-691.

Figure Captions

Fig. 1. Definition of symbols

Fig. 2. Loading conditions of web crippling tests: (a) Interior-One-Flange (IOF) loading; (b) Interior-Two-Flange (ITF) loading; (c) Interior loading (IL)

Fig. 3. Test setup specimens subjected different concentrated interior bearing loads: (a) Specimen IOF150×80×3.0N90; (b) Specimen ITF80×150×3.0N150; (c) Specimen IL100×100×3.0N30

Fig. 4. Load-web deformation curves for specimens under different loading conditions: (a) Load-horizontal deformation; (b) Load-vertical deformation

Fig. 5. Web crippling failure of specimens subjected different concentrated interior bearing loads: (a) Specimen IOF80×150×3.0N60; (b) Specimen ITF80×150×3.0N150; (c) Specimen IL100×100×3.0N30

Fig. 6. Comparison of test strengths with predicted strengths by different provisions: (a) ASCE (2002); (b) EC-1.4 (2015); (c) NAS (2016); (d) Zhou and Young (2008).

Table 1. Measured dimensions and test strengths for specimens under IOF loading condition

Specimen	H (mm)	B (mm)	t (mm)	r_i (mm)	L (mm)	h/t	r_i/t	N/t	N/h	P_{test} (kN)
IOF40×60×2.0N30	40.4	60.2	2.00	1.9	211.3	16.3	0.9	15.0	0.92	31.4
IOF40×60×2.0N60	40.5	60.2	2.02	1.9	300.3	16.2	0.9	29.7	1.83	32.2
IOF50×20×1.5N30	50.1	20.3	1.51	1.0	240.5	29.9	0.7	19.9	0.67	21.1
IOF50×20×1.5N30-r	50.1	20.3	1.57	0.9	240.2	28.8	0.6	19.1	0.66	20.9
IOF60×40×2.0N30	60.2	40.1	2.03	1.9	271.1	25.8	0.9	14.8	0.57	29.3
IOF60×120×3.0N60	60.0	120.0	3.08	3.3	361.1	15.4	1.1	19.5	1.27	73.5
IOF60×120×3.0N90	60.1	120.0	3.07	3.3	450.6	15.5	1.1	29.3	1.90	77.5
IOF80×150×3.0N60	80.2	151.3	3.09	6.5	419.5	19.7	2.1	19.4	0.98	57.7
IOF80×150×3.0N150	80.6	151.6	3.09	6.0	690.0	20.2	1.9	48.5	2.40	70.6
IOF100×100×3.0N30	100.3	100.1	3.09	3.4	389.8	28.3	1.1	9.7	0.34	70.7
IOF100×100×3.0N90	100.3	100.3	3.10	3.5	569.7	28.1	1.1	29.1	1.03	89.1
IOF100×100×3.0N90-r	100.3	100.2	3.10	3.4	570.0	28.2	1.1	29.0	1.03	89.5
IOF120×60×3.0N30	120.1	60.1	3.07	3.6	451.7	34.8	1.2	9.8	0.28	61.1
IOF120×60×3.0N60	120.0	59.7	3.07	3.1	541.2	35.0	1.0	19.5	0.56	71.6
IOF150×80×3.0N30	151.6	80.1	3.08	6.5	539.7	42.9	2.1	9.7	0.23	48.4
IOF150×80×3.0N90	150.7	80.1	3.09	6.2	720.5	42.7	2.0	29.1	0.68	62.1

Table 2. Measured dimensions and test strengths for specimens under ITF loading condition

Specimen	H (mm)	B (mm)	t (mm)	r_i (mm)	L (mm)	h/t	r_i/t	N/t	N/h	P_{test} (kN)
ITF20×50×1.5N30	20.1	50.2	1.56	0.8	90.0	9.8	0.5	19.2	1.95	25.6
ITF20×50×1.5N30-r	20.1	50.1	1.52	1.1	90.3	9.7	0.7	19.7	2.03	26.1
ITF20×50×1.5N50	19.9	50.1	1.50	0.9	110.0	10.1	0.6	33.4	3.32	36.5
ITF40×60×2.0N30	40.3	60.2	2.00	2.0	150.8	16.2	1.0	15.0	0.93	31.4
ITF40×60×2.0N60	40.3	60.2	2.01	1.9	180.8	16.2	0.9	29.9	1.85	39.8
ITF50×20×1.5N30	50.1	20.3	1.49	1.0	180.0	30.3	0.7	20.1	0.66	21.5
ITF50×20×1.5N30-r	50.1	20.3	1.49	1.0	180.0	30.3	0.7	20.1	0.66	21.4
ITF60×40×2.0N30	60.2	40.2	2.02	2.1	209.5	25.7	1.1	14.9	0.58	31.7
ITF60×40×2.0N30-r	60.2	40.2	2.03	1.9	210.8	25.8	0.9	14.8	0.57	31.7
ITF60×120×3.0N60	60.6	120.0	3.05	2.8	240.7	16.1	0.9	19.7	1.22	77.8
ITF60×120×3.0N90	60.0	120.0	3.08	3.3	271.8	15.4	1.1	29.2	1.90	92.0
ITF60×120×3.0N90-r	60.1	119.9	3.09	3.1	265.7	15.4	1.0	29.1	1.89	91.0
ITF80×150×3.0N60	80.8	152.4	3.09	6.5	299.7	19.9	2.1	19.4	0.97	57.3
ITF80×150×3.0N150	80.8	151.0	3.09	6.3	390.2	20.1	2.0	48.6	2.42	78.5
ITF80×150×3.0N150-r	80.0	151.2	3.09	6.5	390.3	19.7	2.1	48.6	2.47	78.9
ITF100×100×3.0N30	100.4	100.1	3.07	3.3	330.0	28.5	1.1	9.8	0.34	72.4
ITF100×100×3.0N90	100.4	100.2	3.10	3.3	390.0	28.3	1.1	29.1	1.03	85.9
ITF120×60×3.0N30	120.2	59.8	3.08	3.3	390.3	34.9	1.1	9.7	0.28	73.4
ITF120×60×3.0N60	119.9	60.2	3.07	2.9	420.8	35.2	0.9	19.5	0.56	78.9
ITF150×80×3.0N30	152.1	80.2	3.08	6.3	479.3	43.3	2.0	9.7	0.22	54.8
ITF150×80×3.0N90	152.1	80.2	3.09	6.5	539.5	43.0	2.1	29.1	0.68	69.6

Table 3. Measured dimensions and test strengths for specimens under IL loading condition

Specimen	H (mm)	B (mm)	t (mm)	r_i (mm)	L (mm)	h/t	r_i/t	N/t	N/h	P_{test} (kN)
IL20×50×1.5N30	20.1	50.2	1.52	1.0	90.3	9.9	0.7	19.8	1.99	29.9
IL20×50×1.5N50	20.1	50.1	1.51	0.9	110.2	10.1	0.6	33.1	3.26	41.1
IL40×60×2.0N30	40.4	60.2	2.03	1.6	151.2	16.3	0.8	14.8	0.91	35.9
IL40×60×2.0N60	40.4	60.2	2.01	1.6	180.8	16.5	0.8	29.9	1.81	48.4
IL40×60×2.0N60-r	40.3	60.2	2.04	1.5	180.4	16.3	0.7	29.4	1.81	48.4
IL50×20×1.5N30	50.1	20.4	1.54	1.0	180.0	29.3	0.7	19.5	0.67	22.2
IL50×20×1.5N30-r	50.1	20.3	1.52	0.8	180.0	29.8	0.5	19.7	0.66	22.3
IL60×40×2.0N30	60.2	40.4	2.05	1.5	210.4	25.9	0.7	14.6	0.56	34.0
IL60×40×2.0N50	60.3	40.3	2.03	1.6	229.7	26.1	0.8	24.6	0.94	40.2
IL60×40×2.0N50-r	60.3	40.4	2.00	1.6	232.1	26.5	0.8	25.0	0.94	39.8
IL60×120×3.0N60	60.3	120.2	3.06	3.3	241.8	15.6	1.1	19.6	1.26	86.6
IL60×120×3.0N120	60.2	119.9	3.06	2.9	300.6	15.8	0.9	39.2	2.48	128.8
IL80×150×3.0N60	80.3	151.2	3.09	6.3	300.0	19.9	2.0	19.4	0.97	65.2
IL80×150×3.0N150	80.3	151.6	3.07	4.5	390.7	21.2	1.5	48.8	2.30	89.3
IL80×150×3.0N150-r	80.8	151.4	3.08	5.8	390.3	20.5	1.9	48.7	2.38	88.7
IL100×100×3.0N30	100.4	100.3	3.08	3.6	330.5	28.3	1.2	9.7	0.34	74.3
IL100×100×3.0N90	100.4	100.2	3.08	4.3	390.0	27.8	1.4	29.2	1.05	102.0
IL120×60×3.0N30	120.1	60.5	3.09	3.1	390.1	34.8	1.0	9.7	0.28	73.4
IL120×60×3.0N60	120.1	60.4	3.06	3.0	421.2	35.3	1.0	19.6	0.56	81.5
IL150×80×3.0N30	151.3	80.8	3.08	6.5	480.2	42.9	2.1	9.7	0.23	55.7
IL150×80×3.0N90	151.3	80.1	3.09	6.3	540.2	42.9	2.0	29.1	0.68	70.3

Table 4. Material properties of LDSS obtained from coupon tests

Section $H \times B \times$ t (mm)	Tensile coupon			Compressive coupon	
	E^T	$f_{0.2}^T$	f_u^T	E^C	$f_{0.2}^C$
	GPa	MPa	MPa	GPa	MPa
20 × 50 × 1.5	194	656	777	-	-
40 × 60 × 2.0	199	600	756	-	-
50 × 20 × 1.5	194	656	777	212	611
60 × 40 × 2.0	199	600	756	211	627
60 × 120 × 3.0	206	620	736	215	727
80 × 150 × 3.0	194	491	722	214	546
100 × 100 × 3.0	202	557	701	209	551
120 × 60 × 3.0	206	620	736	215	611
150 × 80 × 3.0	194	491	722	208	518

Source: Cai and Young (2019).

Table 5. Coefficients for web crippling design of cold-formed steel sections

Reference	Steel	Section type	Load cases	Coefficients					Limits			
				C	C_R	C_N	C_h	ϕ	r_i/t	N/t	h/t	N/h
NAS (2016)	Carbon steel	Single web channel	IOF	13.0	0.23	0.14	0.01	0.90	≤ 5.0	≤ 210	≤ 200	≤ 2.0
			ITF	24.0	0.52	0.15	0.001	0.80	≤ 3.0	≤ 210	≤ 200	≤ 2.0
Zhou & Young (2008)	Duplex stainless steel	Square and rectangular hollow	IOF	7.0	0.21	0.26	0.001	0.70	≤ 2.0	≤ 50	≤ 50	≤ 2.0
			ITF	7.0	0.11	0.24	0.001	0.70	≤ 2.0	≤ 50	≤ 50	≤ 2.0
			IL	15.3	0.26	0.18	0.003	0.80	≤ 2.0	≤ 50	≤ 200	≤ 1.6

Note: The table is suitable to stiffened or partially stiffened flanges that unfastened to support.

Table 6. Comparison of test strengths with predicted strengths under IOF loading condition

Specimen	*Per web*	*Using material properties from tensile coupons*				*Using material properties from compressive coupons*			
	P_{test} (kN)	P_{test}/P_{ASCE}^{T}	P_{test}/P_{EC}^{T}	P_{test}/P_{NAS}^{T}	$P_{test}/P_{Z\&Y}^{T}$	P_{test}/P_{ASCE}^{C}	P_{test}/P_{EC}^{C}	P_{test}/P_{NAS}^{C}	$P_{test}/P_{Z\&Y}^{C}$
IOF40×60×2.0N30	31.4	1.16	2.49	0.88	1.17	-	-	-	-
IOF40×60×2.0N60	32.2	1.06	2.51	0.77	0.98	-	-	-	-
IOF50×20×1.5N30	21.1	1.36	2.65	0.87	1.14	1.36	2.63	0.94	1.22
IOF50×20×1.5N30-r	20.9	1.24	2.43	0.79	1.03	1.24	2.41	0.85	1.11
IOF60×40×2.0N30	29.3	1.06	2.26	0.80	1.07	1.06	2.15	0.77	1.02
IOF60×120×3.0N60	73.5	1.11	2.59	0.81	1.06	1.11	2.34	0.69	0.91
IOF60×120×3.0N90	77.5	1.11	2.75	0.79	1.01	1.12	2.48	0.67	0.86
IOF80×150×3.0N60	57.7	0.98	2.45	0.92	1.18	0.95	2.21	0.83	1.06
IOF80×150×3.0N150	70.6	1.01	2.98	0.90	1.08	0.97	2.69	0.81	0.98
IOF100×100×3.0N30	70.7	1.17	2.64	0.99	1.35	1.17	2.61	1.00	1.37
IOF100×100×3.0N90	89.1	1.31	3.33	1.02	1.28	1.31	3.28	1.03	1.30
IOF100×100×3.0N90-r	89.5	1.31	3.33	1.02	1.28	1.31	3.28	1.03	1.30
IOF120×60×3.0N30	61.1	1.03	2.18	0.79	1.07	1.03	2.15	0.80	1.09
IOF120×60×3.0N60	71.6	1.12	2.53	0.81	1.04	1.12	2.50	0.82	1.05
IOF150×80×3.0N30	48.4	0.91	2.07	0.89	1.18	0.89	1.95	0.85	1.12
IOF150×80×3.0N90	62.1	1.02	2.63	0.92	1.12	1.00	2.47	0.87	1.07
Mean, P_m		1.12	2.61	0.87	1.13	1.12	2.51	0.85	1.10
COV, V_p		0.115	0.135	0.097	0.095	0.130	0.155	0.132	0.134
Resistance factor, ϕ		0.70	0.91	0.90	0.70	0.70	0.91	0.90	0.70
Reliability index, β		3.66	5.45	1.85	3.81	3.52	5.05	1.65	3.44

Table 7. Comparison of test strengths with predicted strengths under ITF loading condition

Specimen	*Per web*	*Using material properties from tensile coupons*				*Using material properties from compressive coupons*			
	P_{test} (kN)	P_{test}/P_{ASCE}^{T}	P_{test}/P_{EC}^{T}	P_{test}/P_{NAS}^{T}	$P_{test}/P_{Z\&Y}^{T}$	P_{test}/P_{ASCE}^{C}	P_{test}/P_{EC}^{C}	P_{test}/P_{NAS}^{C}	$P_{test}/P_{Z\&Y}^{C}$
ITF20×50×1.5N30	25.6	1.17	6.02	0.64	1.21	-	-	-	-
ITF20×50×1.5N30-r	26.1	1.26	6.56	0.78	1.32	-	-	-	-
ITF20×50×1.5N50	36.5	1.79	9.34	0.94	1.63	-	-	-	-
ITF40×60×2.0N30	31.4	0.90	5.05	0.72	1.09	-	-	-	-
ITF40×60×2.0N60	39.8	1.11	6.32	0.76	1.14	-	-	-	-
ITF50×20×1.5N30	21.5	1.16	5.56	0.64	1.12	1.16	5.52	0.69	1.20
ITF50×20×1.5N30-r	21.4	1.15	5.54	0.64	1.12	1.15	5.49	0.69	1.20
ITF60×40×2.0N30	31.7	0.92	5.02	0.74	1.09	0.92	4.77	0.71	1.04
ITF60×40×2.0N30-r	31.7	0.91	4.94	0.68	1.07	0.91	4.69	0.65	1.02
ITF60×120×3.0N60	77.8	0.95	5.58	0.67	1.05	0.95	5.04	0.57	0.89
ITF60×120×3.0N90	92.0	1.09	6.54	0.78	1.10	1.09	5.91	0.66	0.94
ITF60×120×3.0N90-r	91.0	1.07	6.42	0.75	1.08	1.07	5.80	0.64	0.92
ITF80×150×3.0N60	57.3	0.78	4.91	1.25	1.01	0.75	4.44	1.12	0.91
ITF80×150×3.0N150	78.5	1.03	6.73	1.33	1.07	1.00	6.08	1.20	0.96
ITF80×150×3.0N150-r	78.9	1.04	6.79	1.41	1.08	1.00	6.13	1.26	0.97
ITF100×100×3.0N30	72.4	0.94	5.53	0.86	1.28	0.94	5.46	0.87	1.29
ITF100×100×3.0N90	85.9	1.07	6.44	0.81	1.14	1.07	6.36	0.81	1.15
ITF120×60×3.0N30	73.4	0.95	5.22	0.76	1.16	0.95	5.14	0.78	1.17
ITF120×60×3.0N60	78.9	1.01	5.61	0.69	1.05	1.01	5.53	0.70	1.07
ITF150×80×3.0N30	54.8	0.82	4.72	1.30	1.15	0.80	4.44	1.23	1.09
ITF150×80×3.0N90	69.6	1.01	5.96	1.40	1.10	0.99	5.61	1.32	1.05
Mean, P_m		1.05	5.94	0.88	1.15	0.99	5.40	0.87	1.06
COV, V_p		0.197	0.171	0.307	0.117	0.112	0.111	0.302	0.115
Resistance factor, ϕ		0.70	0.91	0.80	0.70	0.70	0.91	0.80	0.70
Reliability index, β		2.89	7.81	1.50	3.74	3.19	8.43	1.45	3.43

Table 8. Comparison of test strengths with predicted strengths under IL loading condition

Specimen	*Per web*	*Using material properties from tensile coupons*						*Using material properties from compressive coupons*					
	P_{test} (kN)	P_{test}/P_{ASCE}^{T}		P_{test}/P_{EC}^{T}	P_{test}/P_{NAS}^{T}		$P_{test}/P_{Z\&Y}^{T}$	P_{test}/P_{ASCE}^{C}		P_{test}/P_{EC}^{C}	P_{test}/P_{NAS}^{C}		$P_{test}/P_{Z\&Y}^{C}$
	IL	IOF	ITF	IL	IOF	ITF	IL	IOF	ITF	IL	IOF	ITF	IL
IL20×50×1.5N30	29.9	1.85	1.46	3.72	1.20	0.86	1.23	-	-	-	-	-	-
IL20×50×1.5N50	41.1	2.36	1.98	5.11	1.46	1.02	1.55	-	-	-	-	-	-
IL40×60×2.0N30	35.9	1.29	1.00	2.75	0.95	0.72	0.96	-	-	-	-	-	-
IL40×60×2.0N60	48.4	1.62	1.35	3.78	1.14	0.86	1.20	-	-	-	-	-	-
IL40×60×2.0N60-r	48.4	1.58	1.31	3.66	1.10	0.81	1.15	-	-	-	-	-	-
IL50×20×1.5N30	22.2	1.38	1.12	2.70	0.89	0.62	0.89	1.38	1.12	2.68	0.95	0.67	0.96
IL50×20×1.5N30-r	22.3	1.40	1.14	2.72	0.88	0.60	0.89	1.40	1.14	2.70	0.95	0.64	0.95
IL60×40×2.0N30	34.0	1.21	0.96	2.55	0.89	0.65	0.88	1.21	0.96	2.42	0.85	0.62	0.84
IL60×40×2.0N50	40.2	1.38	1.14	3.08	0.98	0.73	1.01	1.37	1.14	2.93	0.94	0.70	0.96
IL60×40×2.0N50-r	39.8	1.40	1.17	3.14	1.00	0.75	1.03	1.40	1.16	2.98	0.96	0.72	0.98
IL60×120×3.0N60	86.6	1.33	1.06	3.09	0.97	0.81	1.00	1.33	1.06	2.79	0.82	0.69	0.85
IL60×120×3.0N120	128.8	1.75	1.52	4.57	1.22	0.97	1.31	1.75	1.52	4.12	1.04	0.82	1.12
IL80×150×3.0N60	65.2	1.10	0.88	2.76	1.03	1.34	1.08	1.07	0.85	2.49	0.92	1.20	0.97
IL80×150×3.0N150	89.3	1.25	1.14	3.73	1.09	1.06	1.19	1.21	1.11	3.37	0.98	0.95	1.07
IL80×150×3.0N150-	88.7	1.27	1.15	3.75	1.13	1.34	1.25	1.23	1.12	3.39	1.02	1.21	1.13
IL100×100×3.0N30	74.3	1.24	0.96	2.80	1.06	0.91	1.04	1.25	0.96	2.77	1.07	0.92	1.05
IL100×100×3.0N90	102.0	1.53	1.30	3.88	1.22	1.14	1.29	1.53	1.30	3.84	1.23	1.16	1.30
IL120×60×3.0N30	73.4	1.21	0.94	2.57	0.92	0.74	0.89	1.21	0.94	2.53	0.93	0.75	0.91
IL120×60×3.0N60	81.5	1.28	1.05	2.90	0.92	0.73	0.93	1.28	1.06	2.85	0.93	0.74	0.94
IL150×80×3.0N30	55.7	1.05	0.83	2.38	1.03	1.40	1.02	1.03	0.82	2.24	0.97	1.32	0.97
IL150×80×3.0N90	70.3	1.16	1.01	2.98	1.04	1.33	1.11	1.14	0.99	2.80	0.99	1.26	1.05
Mean, P_m		1.41	1.17	3.27	1.05	0.92	1.05	1.30	1.08	2.93	0.97	0.90	1.00
COV, V_p		0.212	0.223	0.216	0.136	0.276	0.137	0.138	0.159	0.174	0.096	0.278	0.114
Resistance factor, ϕ		0.70	0.70	0.70	0.90	0.80	0.80	0.70	0.70	0.70	0.90	0.80	0.80
Reliability index, β		3.68	3.03	6.05	2.40	1.72	2.80	4.01	3.20	6.22	2.27	1.62	2.75

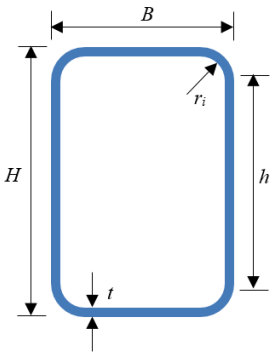

Fig. 1. Definition of symbols

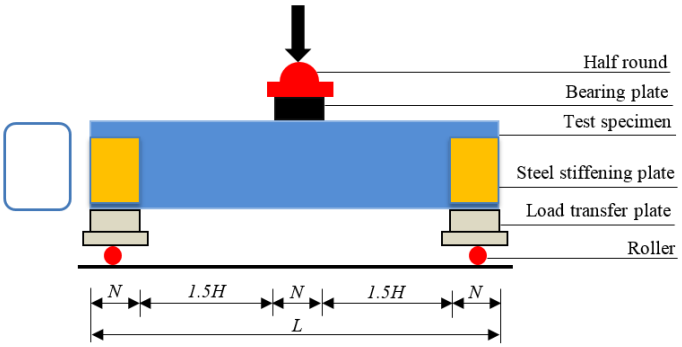

Fig. 2. Loading conditions of web crippling tests
(a) Interior-One-Flange (IOF) loading;

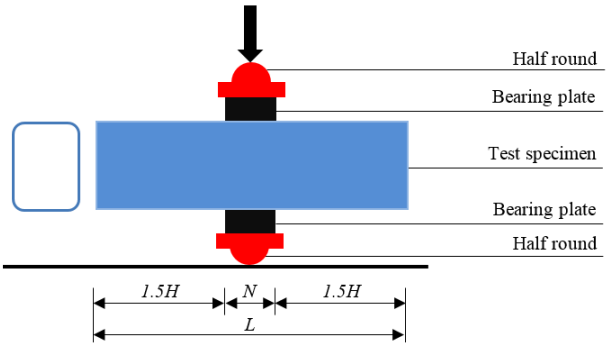

Fig. 2. Loading conditions of web crippling tests
(b) Interior-Two-Flange (ITF) loading

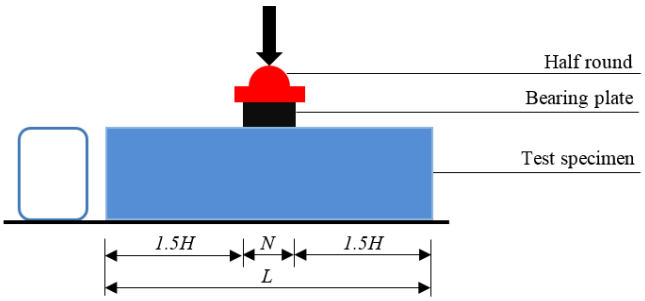

Fig. 2. Loading conditions of web crippling tests
(c) Interior loading (IL)

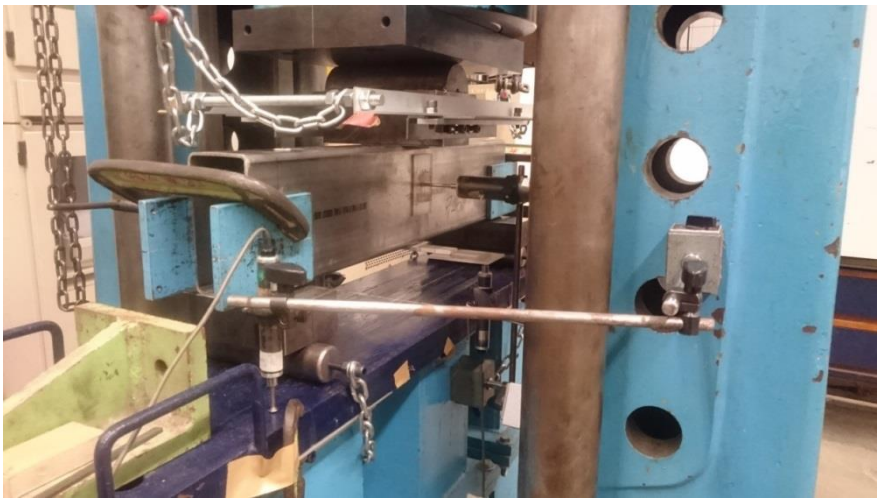

Fig. 3. Test setup specimens subjected different concentrated interior bearing loads
(a) Specimen IOF150×80×3.0N90

Fig. 3. Test setup specimens subjected different concentrated interior bearing loads
(b) Specimen ITF80×150×3.0N150

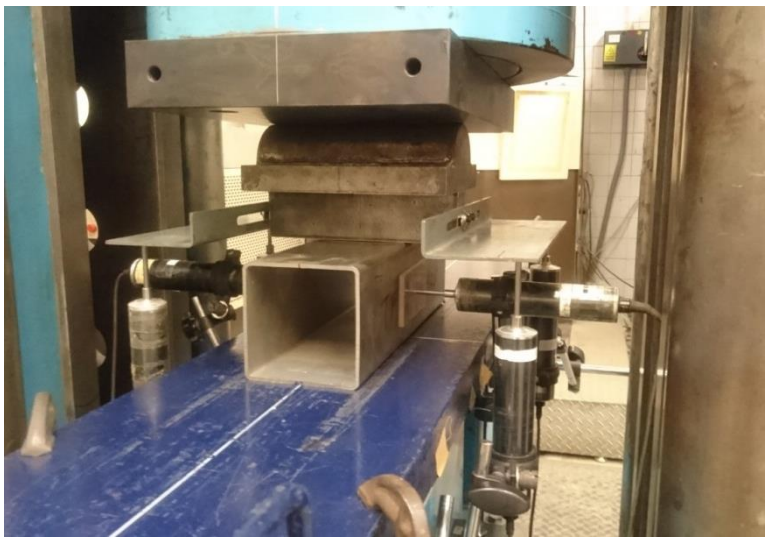

Fig. 3. Test setup specimens subjected different concentrated interior bearing loads
(c) Specimen IL100×100×3.0N30

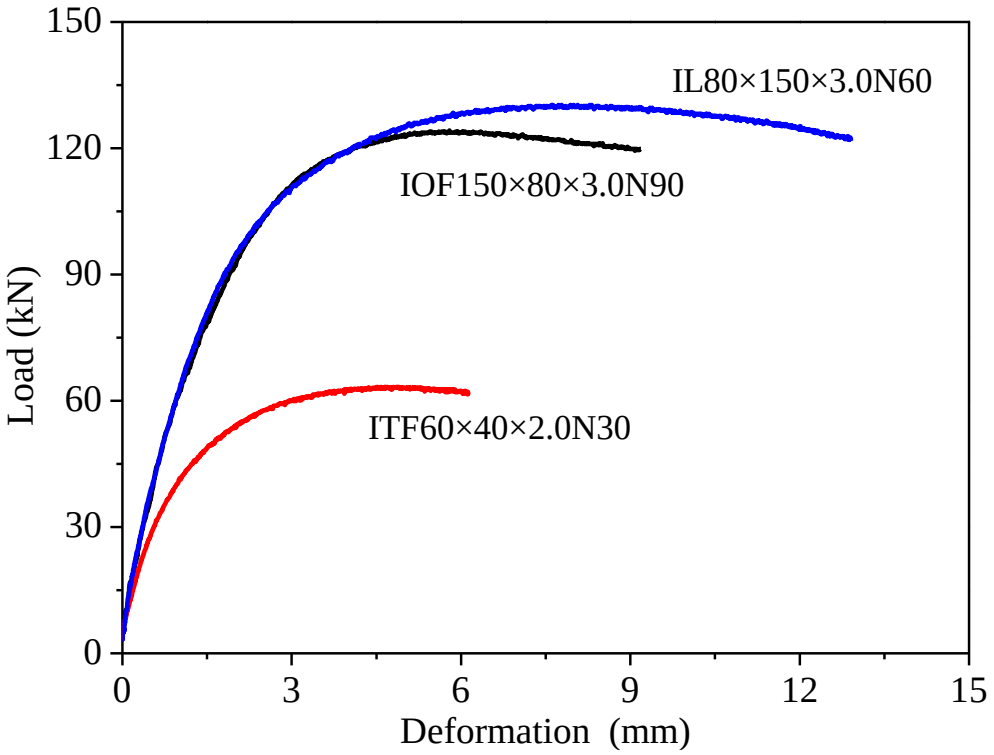

Fig. 4. Load-web deformation curves for specimens under different loading conditions
(a) Load-horizontal deformation

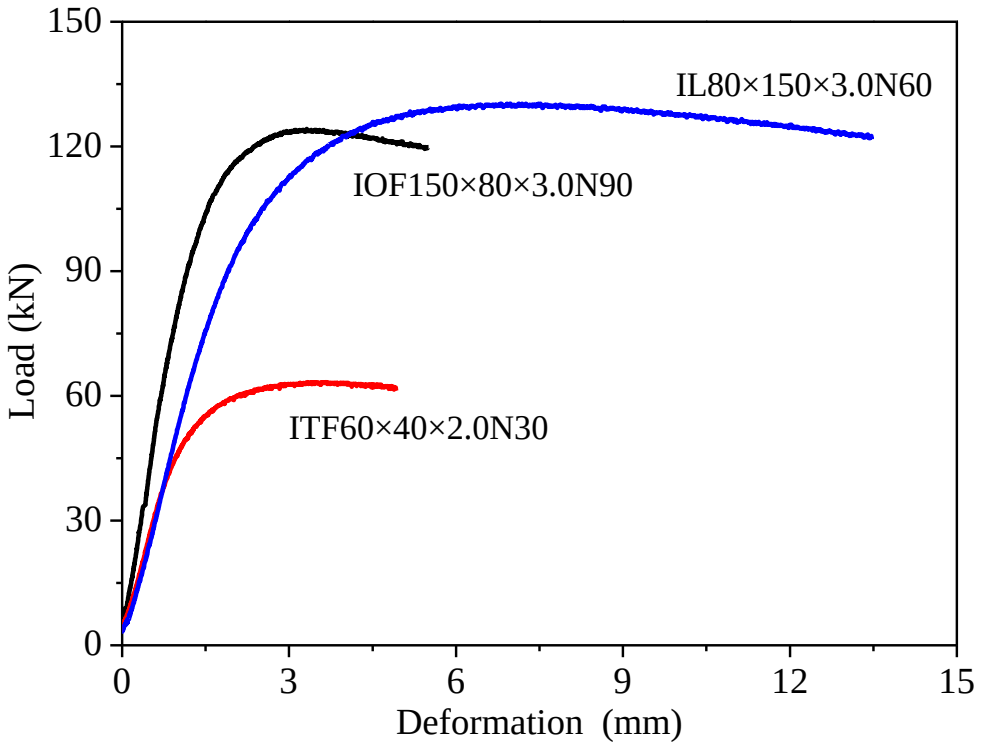

Fig. 4. Load-web deformation curves for specimens under different loading conditions
(b) Load-vertical deformation

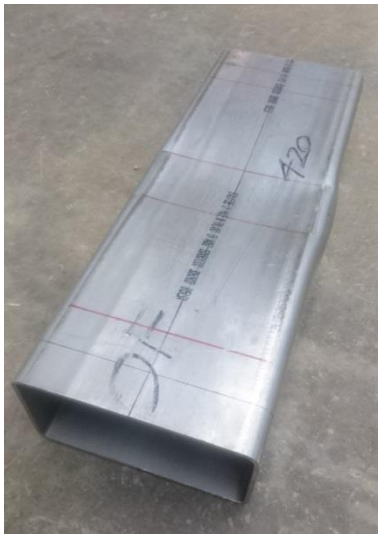

Fig. 5. Web crippling failure of specimens subjected different concentrated interior bearing loads
(a) Specimen IOF80×150×3.0N60

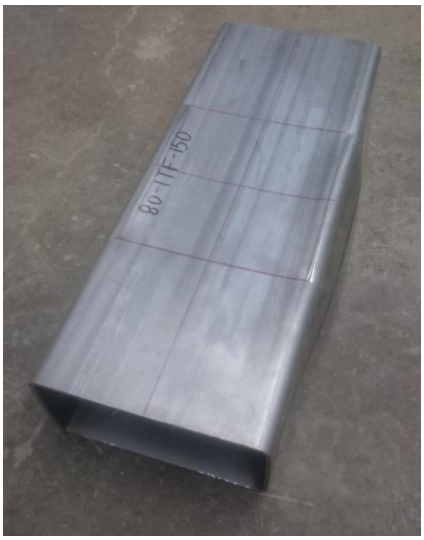

Fig. 5. Web crippling failure of specimens subjected different concentrated interior bearing loads (b) Specimen ITF80×150×3.0N150

Fig. 5. Web crippling failure of specimens subjected different concentrated interior bearing loads (c) Specimen IL100×100×3.0N30

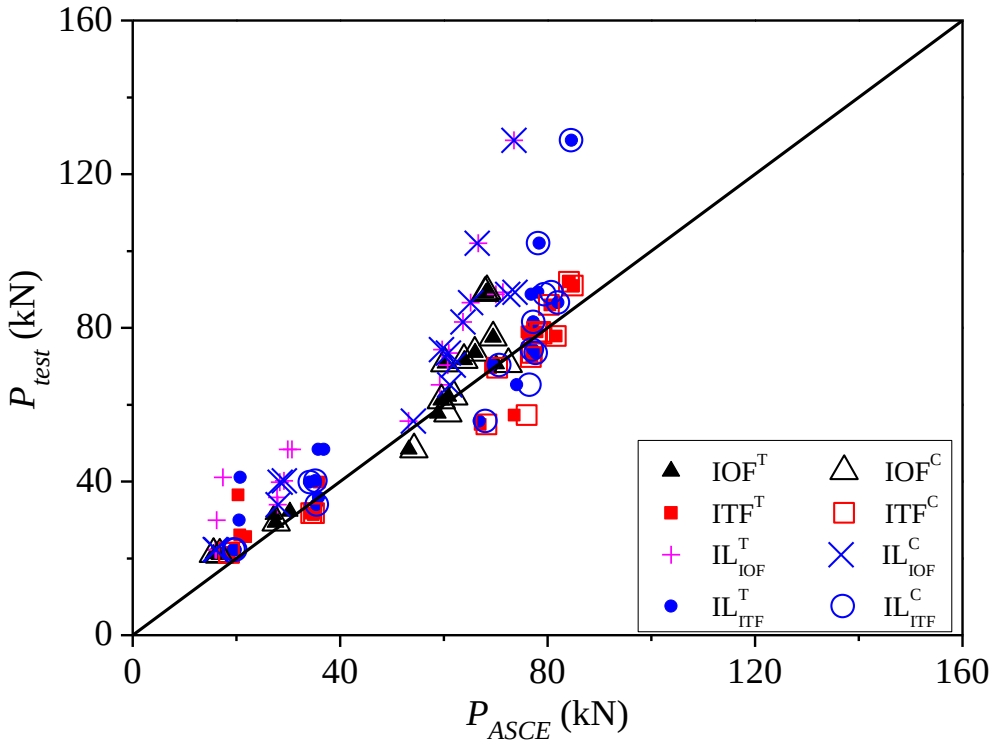

Fig. 6. Comparison of test strengths with predicted strengths by different provisions
(a) Predictions by ASCE Specification (2002)

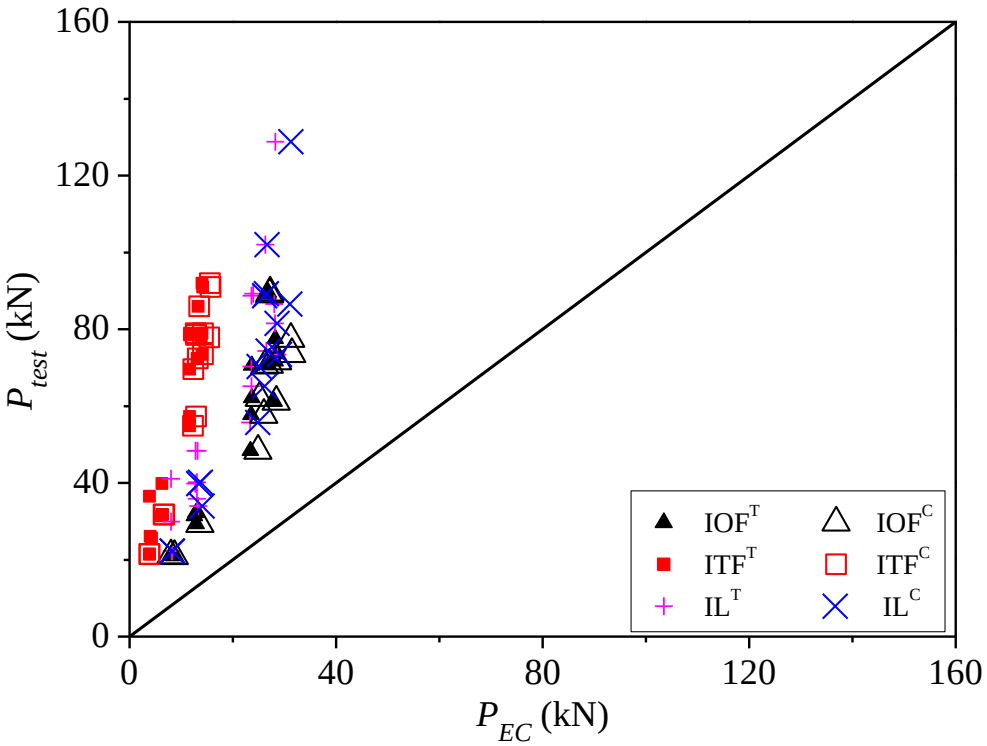

Fig. 6. Comparison of test strengths with predicted strengths by different provisions (b) Predictions by EC-1.4 (2015)

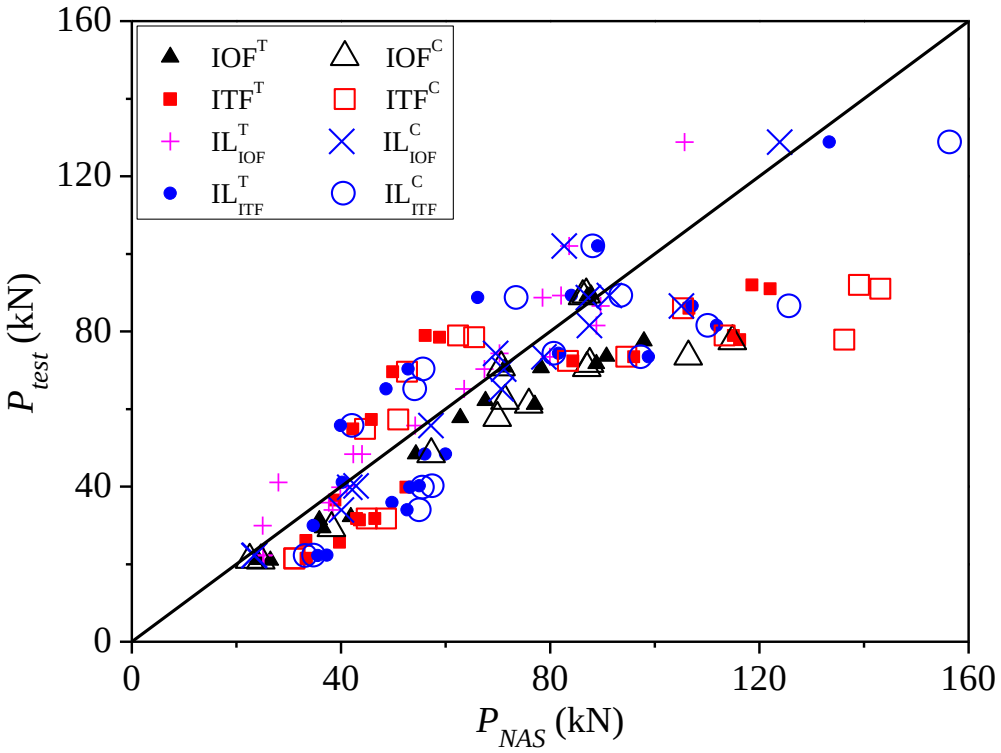

Fig. 6. Comparison of test strengths with predicted strengths by different provisions (c) Predictions by NAS Specification (2016)

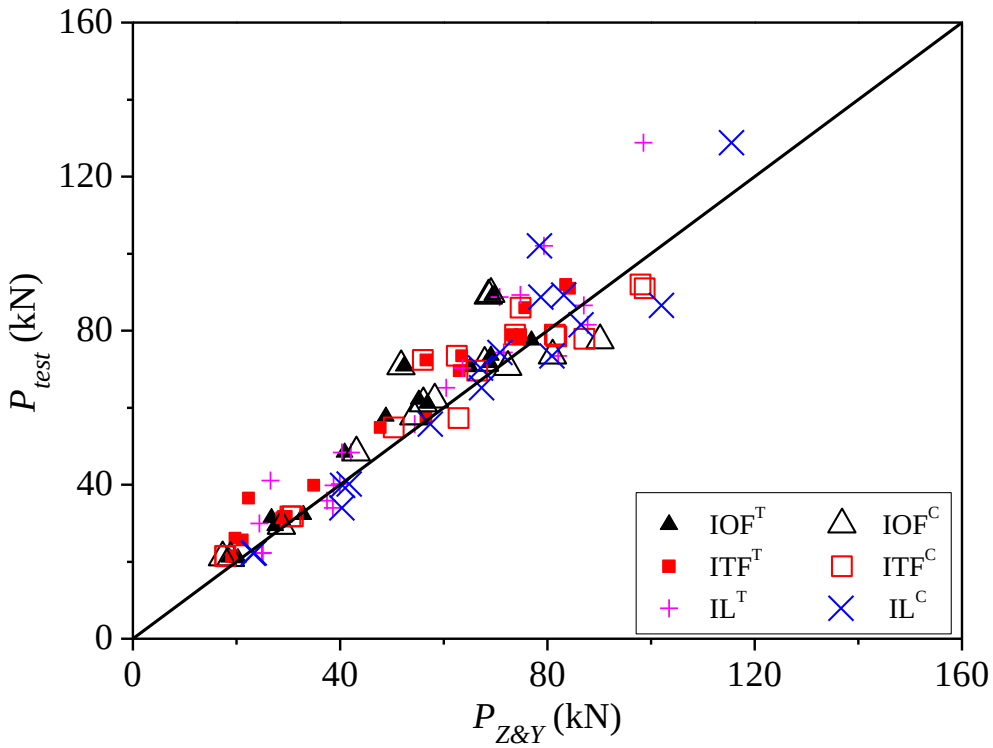

Fig. 6. Comparison of test strengths with predicted strengths by different provisions
(d) Predictions by Zhou and Young (2008)